

HONGYUN CHEN
XIANFENG CHEN[✉]
YISHUAI ZHANG
YUXING XIA

Polarization-dependent coupling in a 1×4 waveguide array in lithium niobate fabricated by femtosecond pulses

Department of Physics, the State Key Laboratory on Fiber Optic Local Area Communication Networks and Advanced Optical Communication Systems, Shanghai Jiao Tong University, 800, Dong Chuan Road, Shanghai 200240, P.R. China

Received: 27 April 2007/Revised version: 29 June 2007
Published online: 17 August 2007 • © Springer-Verlag 2007

ABSTRACT We demonstrate a 1×4 waveguide array produced by an IR femtosecond laser in z -cut lithium niobate (LiNbO_3). The polarization dependence of light coupling in this waveguide structure is experimentally investigated. The coupling constants of the waveguide array are obtained by measuring the ratio of output power of each waveguide for extraordinary rays and ordinary rays, and the variation of coupled power in each waveguide as a function of the waveguide length are demonstrated.

PACS 42.65.Re; 77.84.Dy; 42.82.Et

1 Introduction

Lithium niobate is currently one of the most used crystalline dielectric materials, which is referred to as “silicon in nonlinear optics” because it has excellent acousto-optic, electro-optic, nonlinear optical and optical waveguiding properties [1].

To meet the increasing data capacity requirements in communication systems, there is a growing demand for materials and techniques for fabricating three-dimensional integrated photonic devices. Femtosecond laser fabrication allows the integration of photonic devices in three dimensions. By focusing femtosecond laser pulses inside optical transparent materials, a localized and permanent increase of the refractive index can be achieved. When the sample is moved with respect to the laser beam a refractive index profile as in a buried waveguide can be produced. There have been many reports on using this technique to fabricate waveguide devices in a wide variety of glasses [2–11] and polymers [12–15]. Optical waveguides have also been demonstrated in LiNbO_3 with this technique [16–19]. Gui et al. firstly applied this technique to lithium niobate and demonstrated guiding in the visible spectrum [16]. Thomson et al. identified two different types of waveguide structure that depend on the pulse energy used [17]. Nejadmalayeri et al. generated stable guided-wave optics in bulk lithium niobate that appeared with different processing parameters of pulse duration and polarization [18]. More recently, Burghoff et al. discussed the in-

fluence of the laser parameters and presented results of the thermal, nonlinear and structural properties of the modifications [19]. However, a detailed analysis and further investigations on polarization-dependent coupling in a waveguide array are still missing. Moreover, the coupling constant between waveguides is essential for practical applications of waveguides, unfortunately, it has received little attention in the past years.

In this letter, a 1×4 waveguide array produced by a femtosecond laser in z -cut lithium niobate (LiNbO_3) is presented and characterized. The polarization dependence of light coupling in this waveguide structure is experimentally investigated by changing the polarization of the input laser beam. The coupling constants of the waveguide array for extraordinary rays (c_e) and ordinary rays (c_o) are obtained by the coupled-mode theory.

2 Experiment on the fabrication of a waveguide array

For the fabrication of the waveguide array we used an amplified Ti:sapphire laser system with a central wavelength of 800 nm, a repetition rate of 25 MHz, an on-target laser power of 30 mW and a pulse duration of about 100 fs. The sample was mounted upon a computer-controlled three-axis positioning system. The laser pulses were focused into a polished lithium niobate sample by a long working distance $40 \times$ microscope objective with a numerical aperture of 0.65, and the focal point was located $200 \mu\text{m}$ below the sample surface. The linearly polarized Gaussian laser beam was focused vertically onto the front surface of the sample. All waveguides were fabricated using a single translational scan along the x direction at the speed of $200 \mu\text{m/s}$. The sample we used is a commercial congruent z -cut lithium niobate crystal. A schematic of the setup is given in Fig. 1 and the microscopic image of the top view of the sample is shown in the inset. The 1×4 waveguide array was fabricated with waveguide to waveguide spacing (measured from center to center) of $20 \mu\text{m}$.

3 Results and discussion

For the investigation of the polarization dependent guiding properties of the structure, we rotated a half-wave plate to change the orientation of linearly polarized coupling

✉ Fax: +86-21-54743273, E-mail: xfchen@sjtu.edu.cn

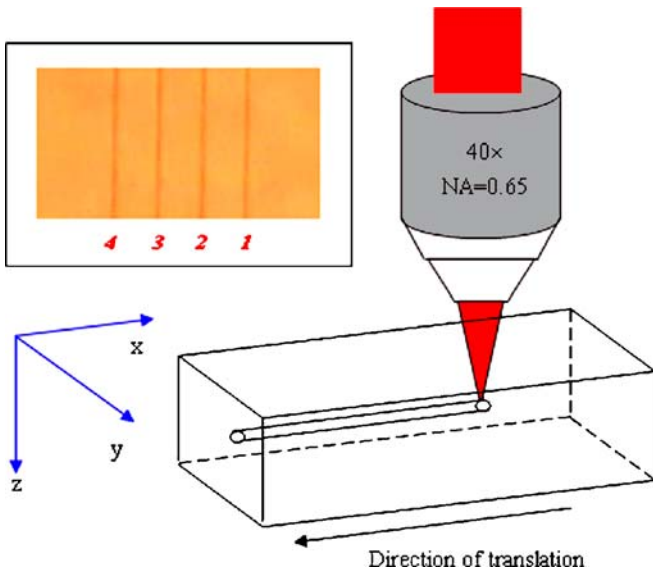


FIGURE 1 Scheme of the writing process in lithium niobate using fs laser pulses. *Inset:* Microscopic image of the top view of the sample of the 1×4 waveguide array marked in arabic numerals

light. The light source is a He-Ne laser light whose wavelength is 632.8 nm. In order to allow the laser beam quality to be substantially improved, a spatial filter was used. The light was coupled into the waveguide marked as 3 as depicted in Fig. 1 with a $10 \times$ microscope objective ($NA = 0.25$), coupled out by a $40 \times$ microscope objective ($NA = 0.65$) objective and projected onto a CCD-camera. A schematic diagram of the setup is shown in Fig. 2. Resulting from the shape of the focal area, the waveguides exhibit an elliptical section with diameters of approximately $2 \times 4 \mu\text{m}^2$. The spatial intensity distributions at the output facet of the 1×4 waveguide array are displayed in Fig. 3. In order to observe the polarization-dependent coupling, we first rotated the half-wave plane to ensure that the orientation of linearly polarized input light was parallel to the z axis, which is the extraordinary light, it can be clearly seen from Fig. 3a that the TM mode was strongly confined. We then rotated the half-wave plane to ensure that the orientation of linearly polarized input light was perpendicular to the z axis, which is the ordinary light, it can

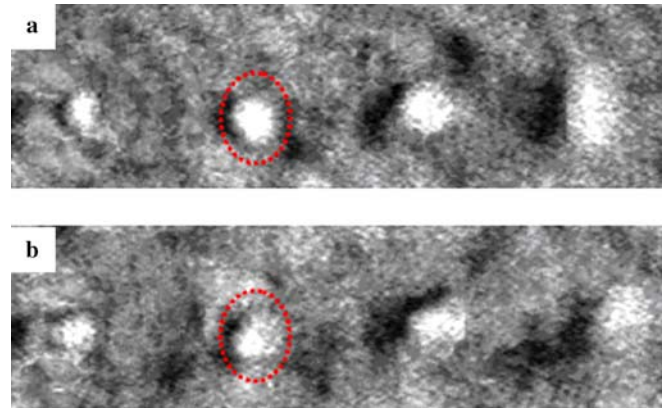


FIGURE 3 Image of the output facet of the 1×4 array sample for TM mode (a) and TE mode (b). The input beam was focused into the waveguide as indicated by the dotted circle

be seen that the TE mode was weakly confined. It is evident that both TM and TE modes are observed in the experiment, and it is shown that the waveguides written by femtosecond laser in lithium niobate are polarization-dependent. We repeated this measurement after one year and found that the coupling behavior changed little. This indicates that our waveguides are more stable than the waveguides reported in [17] which shows stability for 1 month period. In the [19], the modifications show a greatly different behavior in each polarization. In the extraordinary direction, a long filament was created that shows regions of enhanced index at the top and bottom and a region of decreased index in the center (appropriately $0.001 \sim 0.002$). But, the ordinary index only shows the region of decrease. In this case, no waveguiding would occur for ordinary light. Their observations differ from ours in that the light can be guided for both extraordinary and ordinary rays which means the refractive index for both polarizations was increased. The difference in observations may come from the respective repetition rate, the pulse duration and the writing energy of the laser. Further studies need to be carried out to gain a good understanding of these effects.

As shown in Fig. 3, the input light has been coupled to the other waveguides. In order to model the optical responses of the arrays, we use a coupled-mode approach and

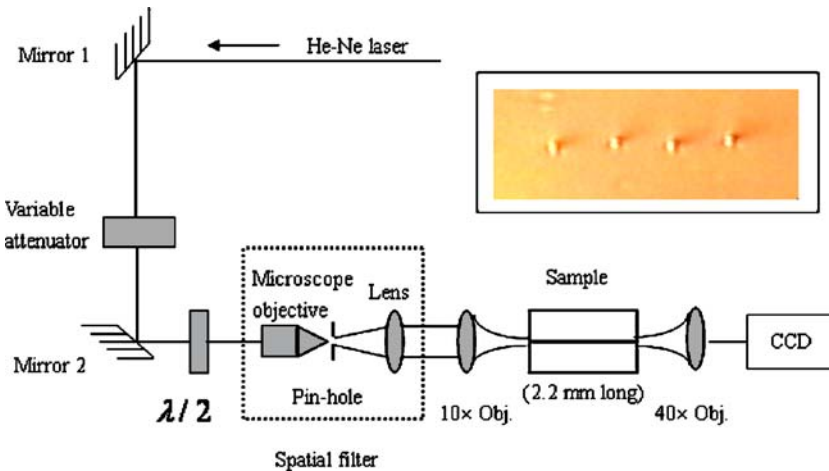


FIGURE 2 Schematic diagram of the experimental setup. A spatial filter was used (the microscope objective is $40 \times$, the diameter of the pin-hole is $25 \mu\text{m}$, the focus length of lens is 50 mm). *Inset:* Microscopic image of the end facet of the sample of the 1×4 waveguide array

consider only the nearest waveguides coupling. The waveguides are marked in the inset in Fig. 1, the amplitudes $a_m(x)$ ($m = 1, 2, 3, 4$) of the electric fields propagating in the waveguides obey the following equations:

$$\begin{cases} i \frac{da_1}{dx} + ca_2 + i\gamma|a_1|^2 a_1 = 0 \\ i \frac{da_2}{dx} + ca_1 + ca_3 + i\gamma|a_2|^2 a_2 = 0 \\ i \frac{da_3}{dx} + ca_2 + ca_4 + i\gamma|a_3|^2 a_3 = 0 \\ i \frac{da_4}{dx} + ca_3 + i\gamma|a_4|^2 a_4 = 0 \end{cases} \quad (1)$$

The coupling between adjacent waveguides induces transverse dynamics. Energy exchange is caused by the overlap of the evanescent tails of the guided modes, which is described by coupling constants for extraordinary rays (c_e) and ordinary rays (c_o) in (1), respectively. The last term describes the nonlinear Kerr effect, with a nonlinear coefficient γ . At low powers, the nonlinear term of (1) can be ignored, the ordinary differential equation is then analytically integrable by solving its eigenvalue equation. The general solution of (1) can be given in the following format:

$$\begin{cases} a_1(x) = c_1 \exp(ik_1cx) - c_2 \exp(ik_2cx) - c_3 \exp(-ik_1cx) \\ \quad + c_4 \exp(-ik_2cx) \\ a_2(x) = k_1(c_1 \exp(ik_1cx) + c_3 \exp(-ik_1cx)) \\ \quad - k_2(c_2 \exp(ik_2cx) + c_4 \exp(-ik_2cx)) \\ a_3(x) = k_1(c_1 \exp(ik_1cx) - c_3 \exp(-ik_1cx)) \\ \quad + k_2(c_2 \exp(ik_2cx) - c_4 \exp(-ik_2cx)) \\ a_4(x) = c_1 \exp(ik_1cx) + c_2 \exp(ik_2cx) + c_3 \exp(-ik_1cx) \\ \quad + c_4 \exp(-ik_2cx) \end{cases} \quad (2)$$

Here $k_1 = \frac{1+\sqrt{5}}{2}$, $k_2 = \frac{-1+\sqrt{5}}{2}$, and c_1, c_2, c_3, c_4 are constants depending on the initial input conditions. If the waveguide marked as 3 in Fig. 1 is excited with unit power, we can obtain the following solution of (1):

$$\begin{cases} a_1(x) = \sqrt{P_3(0)} \frac{1}{\sqrt{5}} (\cos(k_1cx) - \cos(k_2cx)) \\ a_2(x) = \sqrt{P_3(0)} \frac{i}{\sqrt{5}} (k_1 \sin(k_1cx) - k_2 \sin(k_2cx)) \\ a_3(x) = \sqrt{P_3(0)} \frac{1}{\sqrt{5}} (k_1 \cos(k_1cx) + k_2 \cos(k_2cx)) \\ a_4(x) = \sqrt{P_3(0)} \frac{i}{\sqrt{5}} (\sin(k_1cx) + \sin(k_2cx)) \end{cases} \quad (3)$$

Thus, the output powers of the four waveguide are $P(x) = a^*(x)a(x)$. In order to obtain the coupling constant of the extraordinary rays (c_e) and ordinary rays (c_o), the ratios of the output power of waveguides for e rays and o rays were measured by a Si detector after the beams propagate the length of the waveguide L ($L = 2.2$ mm) respectively as follows:

$$\begin{cases} \frac{P_{1e}(L)}{P_{4e}(L)} = \frac{\sin^2(c_e L/2)}{\cos^2(c_e L/2)} = 3.692 \\ \frac{P_{1o}(L)}{P_{4o}(L)} = \frac{\sin^2(c_o L/2)}{\cos^2(c_o L/2)} = 3.529 \end{cases} \quad (4)$$

However, due to the periodicity of the $\arctan(x)$ function, the solutions are not unique. In our calculations, we can achieve multiple solutions of the coupling constant from the power ratio of waveguide #1 to waveguide #4. Then these solutions are employed into (3) to calculate the value of a_2 and a_3 . If the calculated values of a_2 and a_3 is agreeable with the measured power ratio of waveguide #2 (waveguide #3) to waveguide #1, we can conclude that this coupling constant value is reasonable. Otherwise, the solution can be excluded. Therefore, the

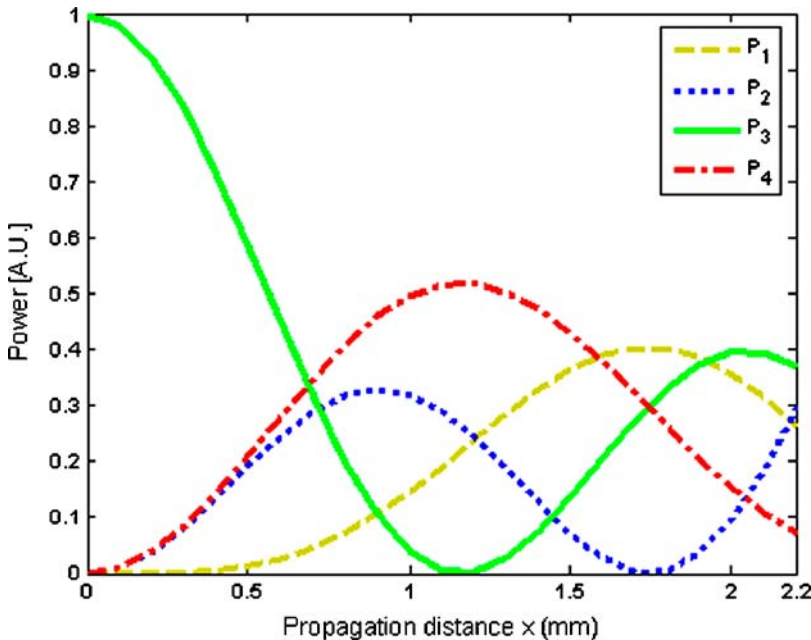


FIGURE 4 The coupled powers of the waveguide as a function of propagation distance x for extraordinary rays

coupling coefficients for extraordinary rays and ordinary rays can be calculated as $c_e = 0.992 \text{ mm}^{-1}$, $c_o = 0.984 \text{ mm}^{-1}$, respectively. In our experiment, an iris is used to filter the noise around the light spot in the measurement. The diameter of the iris remains unchanged during the light power measurement to ensure the same measuring conditions. In addition, a power meter with accuracy of $0.1 \mu\text{W}$ is used. Because the power of light coupled from the waveguides in our experiments ranges from some dozens of microwatts to several hundreds of microwatts, only 1% accuracy can be guaranteed. In order to check the repetition of our measurement, we did the experiments several times and did not find evident change. The different values of coupling coefficients show that waveguiding behaviors for extraordinary rays and ordinary rays are distinct. In order to visualize how the intensity of the four waveguides varies, the relation of power and the propagation distance is plotted by putting the data into (3). Figure 4 shows the output power of each waveguide as a function of propagation distance x when the waveguide marked Arabic numeral 3 was excited for extraordinary rays. For the coupling constants for extraordinary rays and ordinary rays are almost equal ($c_o/c_e = 0.991$), the propagation for ordinary rays in the four waveguides is similar to the extraordinary rays.

4 Conclusion

In conclusion we have demonstrated and characterized a 1×4 waveguide array produced by a femtosecond laser in z -cut lithium niobate. The polarization dependence of light coupling in such waveguide structure is experimentally investigated. From the experimental results, we found that TM mode is stronger confined than TE mode in the 1×4 waveguide array. Using the coupled-mode theory, the coupling constants of the waveguide array through the ratio of output power of each waveguide are achieved. These results

may pave the way for the realization of new applications using femtosecond nonlinear materials processing in LiNbO_3 .

ACKNOWLEDGEMENTS This research was supported by the National Natural Science Foundation of China (No. 60477016 and No.10574092), the Foundation for Development of Science and Technology of Shanghai (No. 04DZ14001) and the National Basic Research Program of China (No. 2006CB806000).

REFERENCES

- 1 A. Yariv, P. Yeh, *Optical Waves in Crystals. Propagation and Control of Laser Radiation* (Wiley, New York, 1984), p. 237
- 2 K.M. Davis, K. Miura, N. Sugimoto, K. Hirao, *Opt. Lett.* **21**, 1729 (1996)
- 3 K. Miura, J. Qiu, H. Inouye, T. Mitsuyu, K. Hirao, *Appl. Phys. Lett.* **71**, 3329 (1997)
- 4 K. Yamada, W. Watanabe, T. Toma, J. Nishii, K. Itoh, *Opt. Lett.* **26**, 19 (2001)
- 5 C.B. Schaffer, A. Brodeur, J.F. Garcia, E. Mazur, *Opt. Lett.* **26**, 93 (2001)
- 6 M. Will, S. Nolte, B.N. Chichkov, A. Tünnemann, *Appl. Opt.* **41**, 4360 (2002)
- 7 M. Streltsov, N.F. Borrelli, *Opt. Lett.* **26**, 42 (2001)
- 8 W. Watanabe, T. Asano, K. Yamada, K. Itoh, J. Nishii, *Opt. Lett.* **28**, 2491 (2003)
- 9 T. Pertsch, U. Peschel, F. Lederer, J. Burghoff, M. Will, S. Nolte, A. Tünnemann, *Opt. Lett.* **29**, 468 (2004)
- 10 Y. Nasu, M. Kohtoku, Y. Hibino, *Opt. Lett.* **30**, 723 (2005)
- 11 H. Chen, X. Chen, Y. Xia, D. Liu, Y. Li, Q. Gong, *Opt. Express* **15**, 5445 (2007)
- 12 Y. Li, K. Yamada, T. Ishizuka, W. Watanabe, K. Itoh, Z. Zhou, *Opt. Express* **10**, 1173 (2002)
- 13 P.J. Scully, D. Jones, D.A. Jaroszynski, *J. Opt. A* **5**, S92 (2003)
- 14 K. Yamasaki, S. Juodkakis, M. Watanabe, H.-B. Sun, S. Matsuo, H. Misawa, *Appl. Phys. Lett.* **76**, 1000 (2000)
- 15 A. Zoubir, C. Lopez, M. Richardson, K. Richardson, *Opt. Lett.* **29**, 1840 (2004)
- 16 L. Gui, B. Xu, T.C. Chong, *IEEE Photon. Technol. Lett.* **16**, 1337 (2004)
- 17 R.R. Thomson, S. Campbell, I.J. Blewett, A.K. Kar, D.T. Reid, *Appl. Phys. Lett.* **88**, 111109 (2006)
- 18 A.H. Nejadmalayeri, P.R. Herman, *Opt. Lett.* **31**, 2987 (2006)
- 19 J. Burghoff, H. Hartung, S. Nolte, A. Tünnemann, *Appl. Phys. A* **86**, 165 (2007)